AAC
Journals.ASM.org

Assessment of Efficacy of Antifungals against *Aspergillus fumigatus*: Value of Real-Time Bioluminescence Imaging

Célimène Galiger,[a] Matthias Brock,[b] Grégory Jouvion,[c] Amélie Savers,[a] Marianna Parlato,[a] Oumaïma Ibrahim-Granet[a]

Institut Pasteur Unité de Recherche Cytokines & Inflammation, Paris, France[a]; Friedrich Schiller University Jena, Institute for Microbiology, and Leibniz Institute for Natural Product Research and Infection Biology, Hans Knoell Institute, Research Group Microbial Biochemistry and Physiology, Jena, Germany[b]; Institut Pasteur, Unité Histopathologie Humaine et Modèles Animaux, Département Infection et Epidémiologie, Paris, France[c]

***Aspergillus fumigatus* causes life-threatening infections, especially in immunocompromised patients. Common drugs for therapy of aspergillosis are polyenes, azoles, and echinocandins. However, despite *in vitro* efficacy of these antifungals, treatment failure is frequently observed. In this study, we established bioluminescence imaging to monitor drug efficacy under *in vitro* and *in vivo* conditions. *In vitro* assays confirmed the effectiveness of liposomal amphotericin B, voriconazole, and anidulafungin. Liposomal amphotericin B and voriconazole were fungicidal, whereas anidulafungin allowed initial germination of conidia that stopped elongation but allowed the conidia to remain viable. *In vivo* studies were performed with a leukopenic murine model. Mice were challenged by intranasal instillation with a bioluminescent reporter strain (5×10^5 and 2.5×10^5 conidia), and therapy efficacies of liposomal amphotericin B, voriconazole, and anidulafungin were monitored. For monotherapy, the highest treatment efficacy was observed with liposomal amphotericin B, whereas the efficacies of voriconazole and anidulafungin were strongly dependent on the infectious dose. When therapy efficacy was studied with different drug combinations, all combinations improved the rate of treatment success compared to that with monotherapy. One hundred percent survival was obtained for treatment with a combination of liposomal amphotericin B and anidulafungin, which prevented not only pulmonary infections but also infections of the sinus. In conclusion, combination therapy increases treatment success, at least in the murine infection model. In addition, our novel approach based on real-time imaging enables *in vivo* monitoring of drug efficacy in different organs during therapy of invasive aspergillosis.**

Aspergillus fumigatus is the main cause of invasive aspergillosis in immunocompromised patients. A review of 595 patients with proven or probable invasive aspergillosis identified a high rate of treatment failure for a wide range of antifungal drugs (36%), with only 27% of treated patients demonstrating a complete response to treatment (1). While in some cases failure of treatment may result from low susceptibility of the pathogen to the respective antifungal, restricted delivery to the site of infection may be another reason for a limited treatment response (2). Therefore, practice guidelines addressing treatment choices support the aggressive use of different drugs, including amphotericin B and its lipid formulation as well as different azoles, including itraconazole, voriconazole, and posaconazole, at the highest recommended doses (3).

The development of a number of antifungals with increased potency and lower toxicity has raised optimism that outcomes of invasive fungal infections can be improved. The availability of liposomal formulations of amphotericin B, azoles with an extended spectrum against filamentous fungi, and a new class of antifungal agents, the echinocandins, confronts the clinician with a widened range of therapeutic choices. Recent clinical trials have provided important insights into how these agents should be used. In particular, voriconazole has demonstrated superior efficacy to amphotericin B in the management of invasive aspergillosis (4), posaconazole has been shown to have significant efficacy in the prophylaxis of invasive fungal infection in high-risk individuals and plays a role in salvage therapy of invasive aspergillosis (4), and caspofungin has demonstrated efficacy in salvage therapy of invasive aspergillosis. In addition, each of the echinocandins shows activity without significant toxicity in therapy of invasive candidiasis (5, 6). Nevertheless, many therapeutic areas of uncertainty remain, including the role of combination therapy, and such approaches will provide the focus for future studies (4).

Due to the difficulties in treating invasive aspergillosis, it remains challenging to gain new insights into the establishment and dissemination of infection. Several murine infection models have been established in recent years to identify virulence determinants which allow *A. fumigatus* to act as a pathogen (7). It is well accepted that compromised immune defense mechanisms on the host side are generally required to allow fungal tissue invasion (8). This is also reflected in murine infection models, where high doses of conidia applied to the respiratory tract are well tolerated only by immunocompetent individuals (9, 10).

In infection models used nowadays for studying the development of invasive aspergillosis, conidia are generally applied intranasally or directly to the trachea by using either a suspension or an aerosol (11). These treatments are believed to resemble most closely the natural route of infection as it occurs in immunosuppressed patients. However, due to uncertainties about correct lung infection, drug testing frequently uses intravenous infections resulting in systemic organ infections whereby the natural primarily

Received 10 August 2012 Returned for modification 10 November 2012
Accepted 11 April 2013
Published ahead of print 15 April 2013
Address correspondence to Oumaïma Ibrahim-Granet, oumaima.granet@pasteur.fr.
C.G. and M.B. contributed equally to this article.

doi:10.1128/AAC.01660-12

challenged target organ, the lung, remains virtually pathogen free. To overcome problems in monitoring a successful infection process, *in vivo* imaging systems provide valuable tools.

In recent years, noninvasive bioluminescence imaging (BLI) has evolved as a powerful technique for studying the establishment and manifestation of infection by pathogens and has provided new insights into the onset and dissemination of infections (12, 13). In conventional animal models used for decades to study experimental aspergillosis, mice were sacrificed at certain time points and investigated by histopathology to confirm the progression of infection. The drawbacks of this method are the time-consuming sample preparation and the selection of organs from animals that are either moribund or sacrificed at a predefined time point, which only provides a snapshot of the infection process rather than giving insights into disease progression. The main advantage of the *in vivo* bioluminescence imaging technique is that real-time monitoring of the spatial and temporal progression of infection can be achieved on single individual animals, without the need to sacrifice the animals at a certain time point (12–14). By using BLI, new insights into the infection process can be gained, accompanied by the possibility to significantly reduce the number of animals in studied cohorts.

The first attempt at *in vivo* monitoring by BLI of pathogenesis caused by a fungal species in a murine infection model was performed on *Candida albicans*. In that study, constitutive luciferase gene expression was enforced by use of the *ENO1* promoter (15), and vaginal mucosal infections were successfully monitored. Additionally, the use of the antifungal drug miconazole revealed a treatment-dependent reduction of bioluminescence which coincided with a decrease in the fungal load (16). However, in a model of *Candida*-mediated sepsis, only weak bioluminescence signals were detected from deep tissues, and emission intensities did not correlate with fungal loads. This result was attributed to a change in the morphology from yeast to hyphal growth, in which production of hydrophobic surface proteins and cell clumping might have interfered with the uptake of the D-luciferin substrate (16).

However, to adapt the BLI technique to filamentous fungi and to confirm that systemic infection can be monitored, we previously generated a bioluminescent *A. fumigatus* strain by genomic integration of the firefly luciferase gene under the control of the constitutively active glyceraldehyde-3-phosphate dehydrogenase promoter. The strain turned out to be an excellent tool for following the manifestation of infection after application of conidia by either an intravenous or intranasal route of infection, as visualized by real-time monitoring of disease progression in murine infection models. In this case, BLI analysis of intranasal infection reflected the progression of pulmonary aspergillosis dependent on the underlying immune response (17, 18). By using the intravenous route of infection, dissemination of *A. fumigatus* dependent on the host immune status was successfully monitored. BLI thereby visualized the heterogeneity of targeted organs dependent on immune status, and the luminescence correlated well with histopathology. These studies confirmed the general suitability of the method to study the infection processes of pathogenic filamentous fungi (19).

The aim of this study was the evaluation of treatment efficacies of various antifungals, such as liposomal amphotericin B, anidulafungin, and voriconazole, either alone or in combination. To enhance the sensitivity of the system, a codon-optimized luciferase gene was synthesized and used for reporter strain construction. With this strain, we examined the effects of the drugs on the germination of conidia under *in vitro* conditions and followed disease progression *in vivo* after intranasal infection of leukopenic cyclophosphamide-treated mice.

MATERIALS AND METHODS

Antifungal drugs. (i) LAmB. AmBisome (LAmB; Gilead Sciences, Inc., San Dimas, CA), a lyophilized liposomal preparation of amphotericin B, was reconstituted in sterile water to a final concentration of 5 mg/ml for injection. The resulting solution of liposomal amphotericin B was further diluted to 2.5 mg/ml to reach a concentration of 10 mg/kg of body weight in sterile 5% dextrose for intraperitoneal (i.p.) injection.

(ii) VOR. In this study, we used two formulations of voriconazole (VOR) (Vfend; Pfizer): (i) a powder (CAS number 137234-62-9; also known as PF-579 955) that is soluble in dimethyl sulfoxide (DMSO) for *in vitro* assays and (ii) a lyophilized preparation of voriconazole reconstituted to 10 mg/ml. The latter solution of voriconazole was further diluted to 2.5 mg/ml to reach a concentration of 10 mg/kg in sterile 5% dextrose for intraperitoneal injection.

(iii) ANI. As for voriconazole, we used two different formulations of anidulafungin (ANI) (Ecalta; Pfizer): (i) a powder (CAS number 166663-25-8; also known as PF-3910960) that is soluble in DMSO and ethanol for *in vitro* testing and (ii) Ecalta (100 mg soluble drug in 20% alcohol) diluted to a concentration of 10 mg/ml. The resulting 10-mg/ml solution of anidulafungin was further diluted to either 2.5 or 1.25 mg/ml to reach a concentration of 5 or 10 mg/kg in sterile 5% dextrose for intraperitoneal injection.

Construction of *A. fumigatus* strain 2/7/1 containing the codon-optimized *Photinus pyralis* luciferase gene luc_{Opt}. *A. fumigatus* strain C3 was used in previous studies (17–19) and contains a *P. pyralis* luciferase gene from plasmid pSP-luc$^+$ that is codon adapted to mammalian cells. To improve luciferase production levels accompanied by an increase in light emission, a synthetic codon-optimized version of the luciferase gene was generated (GenBank accession number KC677695). For this purpose, the amino acid sequence of the luciferase was back translated into the DNA sequence by applying the *A. fumigatus* codon usage table (http://www.kazusa.or.jp/codon/cgi-bin/showcodon.cgi?species=5085&aa=1&style=N). This codon-optimized luc_{Opt} gene, flanked by BamHI and HindIII restriction sites, was synthesized by GenScript Corporation (Piscataway, NJ) and was obtained subcloned into the standard vector pUC19. The vector was linearized with BamHI, and the *gpdA* promoter from *A. fumigatus* was ligated after BglII excision from vector pJETPgpdAAf (17). The correct orientation of the promoter was confirmed by PCR. The *gpdA* promoter additionally contained a NotI restriction site at its 5′ end that allowed the introduction of the pyrithiamine resistance cassette *ptrA*, which was excised from plasmid NotptrA/pJet (17). The resulting plasmid, PgpdAAf/luc_{Opt}/ptrApUC, was used for transformation of *A. fumigatus* strain CBS144.89 by the same procedure as that previously described (17). Twenty transformants were repeatedly streaked on pyrithiamine-containing plates to obtain pure transformants. Conidia were harvested and checked for bioluminescence in a microplate assay (17) in which the bioluminescent strain C3 served as a control. Strains displaying the strongest luminescence signals were selected for Southern analysis with a digoxigenin-labeled probe against the codon-optimized luciferase gene (data not shown). Strain 2/7/1 contained two genomic luc_{Opt} integrations and displayed no growth defects under various *in vitro* cultivation conditions (different temperatures and carbon sources), and it was thus selected for subsequent analyses.

***In vitro* antifungal susceptibility analysis by use of MIC test strips and the microdilution method.** MIC test strips with amphotericin B, anidulafungin, caspofungin, posaconazole, and voriconazole were purchased from bioMérieux (Etest, Nürtingen, Germany). Analyses were performed by a previously described method (20). In brief, to analyze the susceptibility of the parental *A. fumigatus* wild-type strain CBS144.89 and the bioluminescent reporter strain 2/7/1, conidia were freshly harvested in phosphate-buffered saline (PBS)–0.05% Tween 80 from malt extract agar

slants. Conidial suspensions were filtered through a 40-μm cell strainer (BD Biosciences, Heidelberg, Germany) and washed in sterile PBS. Conidium concentrations were determined using a Neubauer chamber and then adjusted to 1×10^6 conidia/ml. A sterile cotton swab was used to streak conidial suspensions in three directions on MOPS (morpholinepropanesulfonic acid)-buffered (pH 7.0) RPMI 1640 (Sigma-Aldrich GmbH, Taufkirchen, Germany) agar plates with 2% glucose. Plates were air dried prior to application of MIC test strips. Plates were incubated at 37°C, and MIC values were determined after 24 and 48 h. Independent duplicates were analyzed for all drugs and strains. To test the susceptibility against amphotericin B, voriconazole, and anidulafungin in liquid medium, a microdilution method for conidium-forming molds (EUCAST E. Def 9.1, July 2008) was followed (21). Appropriate stock solutions were prepared in the recommended solvent (water or DMSO), and dilutions were prepared as recommended in the EUCAST protocol to give final drug concentrations of 0.0624 to 32 mg/liter in 100 μl of double-strength RPMI–2% glucose medium. Antifungal dilutions were transferred to wells of a 96-well flat-bottom microplate. Subsequently, 100 μl of fresh spore suspension containing 2.5×10^5 conidia/ml was added to each well, resulting in a drug concentration in the range of 0.0312 to 16 mg/liter. All drug dilutions were tested in triplicate, including positive (no drugs) and negative (no drugs, no conidia) controls. Plates were incubated at 37°C and read after 48 h. For amphotericin B and voriconazole, MIC values were determined from the last dilution that completely inhibited colony formation. For anidulafungin, the minimal effective concentration (MEC value) was determined by analyzing colony morphology by microscopic evaluation using an inverse microscope (Zeiss Axiovert 40 CFL). To test the combinatorial effects of different drugs, sub-MIC levels of the respective drugs were combined and tested by the microdilution method (21). The tested combinations included amphotericin B at a fixed final concentration of 0.25 mg/liter in combination with either voriconazole or anidulafungin in the range of 0.0312 to 0.25 mg/liter (final concentration). Additionally, voriconazole was used at a fixed final concentration of 0.0625 mg/liter, and then amphotericin B (final concentration range, 0.0625 to 0.5 mg/liter) or anidulafungin (final concentration range, 0.0312 to 0.25 mg/liter) was added. Growth and morphology were evaluated microscopically after 48 h of incubation at 37°C. Synergistic or antagonistic effects were evaluated by comparing growth and growth morphology against the phenotypes observed for the respective drugs in single use.

***In vitro* studies of antifungal drug efficacy by microscopic analysis and bioluminescence detection.** *In vitro* susceptibility of strain 2/7/1 in liquid cultures against antifungals was determined by seeding 5×10^5 conidia in wells of a 24-well plate. Each well contained 500 μl of RPMI 1640 cell culture medium (Invitrogen, Gibco, France) supplemented with 10% fetal calf serum (complete RPMI). Antifungal drugs were added at different concentrations and at the time points indicated in the specific experiments. Plates were incubated for 10 h at 37°C, and conidial germination was determined using an inverted microscope equipped with a Zeiss D1 AxioCam camera (Carl Zeiss SAS, Le Pecq, France). Images were analyzed by using ImageJ software for Windows, which allows calculations of the diameters of conidia and the lengths of *A. fumigatus* hyphae.

After microscopic evaluation, 5 μl PBS containing 0.16 mg of D-luciferin was added to each well, and plates were incubated for 10 min prior to luminescence acquisition on an IVIS 100 system (PerkinElmer, Boston, MA). Photons were collected for 1 min on the high-sensitivity setting. Bioluminescence images were analyzed and the light emission (total photons flux/s) from a region of interest (ROI) quantified with Living Image software (version 3.1; PerkinElmer). Experiments were repeated twice for each concentration, and cultures were made in triplicate.

Murine infection and *in vivo* bioluminescence imaging using an IVIS 100 system. Throughout this study, male BALB/cJ mice (23 to 28 g, 8 weeks old) were used and supplied by the breeding center R. Janvier (Le Genest Saint-Isle, France). Mice were cared for in accordance with Institut Pasteur guidelines, in compliance with European animal welfare regulation. Upon arrival, animals were placed in isolated ventilated cages in groups of five mice. Four and one day before infection (D−4 and D−1, respectively), each mouse received an immunosuppressive regimen by i.p. injection of 200 μl cyclophosphamide (4 mg/ml). Mice were weighed daily to monitor changes in body weight. Mice were marked with dots on the tail to facilitate the distinction between individual mice within the same group. Immediately prior to infection, antifungal drugs were administered by i.p. injection at the indicated concentrations in a final volume of 100 μl. Mice were then anesthetized by intramuscular injection of 150 μl of a solution containing 10 μg/ml ketamine and 10 μg/ml xylazine. Mice were inoculated intranasally with a dose of either 2.5×10^5 or 5×10^5 conidia in 25 μl of PBS. Infected control mice were treated with placebo (5% solution of glucose or 20% ethanol diluted in 5% glucose). The numbers of animals in high-infectious-dose groups were as follows: placebo controls, 15; liposomal amphotericin B, 15; voriconazole, 10; and anidulafungin, 10. The numbers of animals in low-infectious-dose groups were as follows: placebo controls, 25; liposomal amphotericin B, 10; voriconazole, 20; and anidulafungin, 20. The numbers of animals in groups receiving combination therapy at low infectious doses were as follows: liposomal amphotericin B plus anidulafungin, 15; liposomal amphotericin B plus voriconazole, 10; and voriconazole plus anidulafungin, 10. Bioluminescence imaging was started 24 h after infection and was continued on a daily basis. Images were acquired using an IVIS 100 system as previously described (17). In general, each experiment lasted up to 20 days, including 10 days of daily treatment followed by 5 to 10 days without treatment to monitor weight recovery and the complete disappearance of the infection by bioluminescence imaging. At the end of the observation period, surviving animals were euthanized and their organs removed for histological examination.

Histopathology. Histopathologic analysis was performed on mice challenged with the low-dose inoculum (2.5×10^5 conidia). Placebo-treated control mice were analyzed from the day of euthanasia due to severe signs of disease (3 to 6 days after infection). In contrast, mice from the treatment groups were analyzed either from the day they succumbed to infection due to treatment failure or when sacrificed at the end of the observation period. Lungs were immediately fixed in 4% neutral buffered formalin and embedded in paraffin. Five-micrometer sections were cut and stained with hematoxylin and eosin (HE) to visualize immune effector cells or with Grocott's methenamine silver stain (GMS) for detection of fungi (22).

Statistical analyses. (i) *In vitro* tests. The luminescence values of the different cultures in the presence of the antifungals were compared to those of the control cultures by one-way analysis of variance (ANOVA) followed by Dunnett's multiple-comparison test.

(ii) *In vivo* tests. Analyses of survival rates were performed by creating Kaplan-Meier plots and then performing log rank tests (GraphPad Prism). All results are expressed as means ± standard errors (SE), and comparisons for survival studies were considered significant if the P value was <0.05.

Comparisons of body weights and luminescence within the different groups of mice were performed using two-way ANOVA followed by the Bonferroni posttest. All tests were performed using GraphPad Prism 5 software.

RESULTS

Bioluminescence of the *A. fumigatus* reporter strain 2/7/1 carrying a codon-optimized luciferase gene. In order to increase the sensitivity of the bioluminescence-based reporter system, the firefly luciferase gene was codon adapted to the usage of *A. fumigatus*. As in the previously generated reporter strain C3 (17), expression of this new synthetic luciferase gene (luc_{Opt}) was controlled by the *gpdA* promoter from *A. fumigatus*. After transformation of the wild-type strain CBS144.89, transformants were prescreened for bioluminescence, and strain 2/7/1 was selected for further experiments because it showed bright luminescence but no other phe-

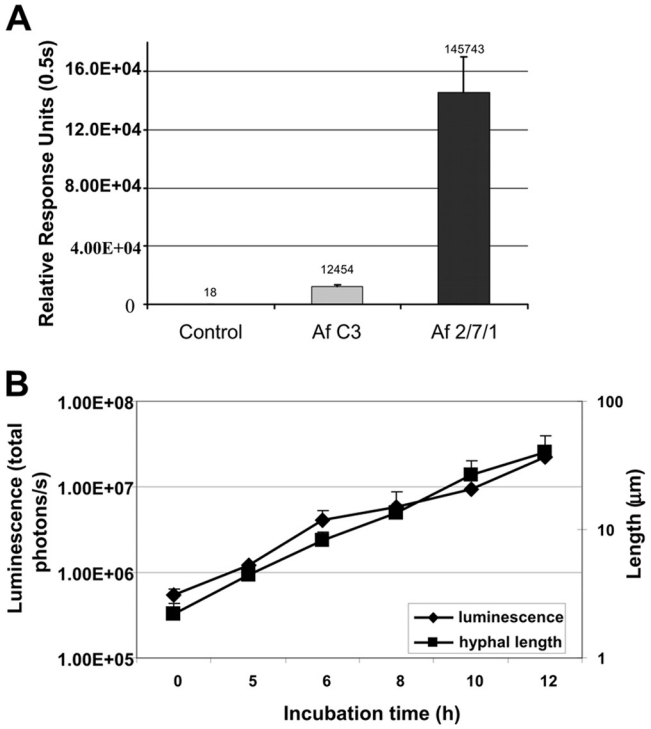

FIG 1 Growth and bioluminescence of *A. fumigatus* strains. (A) Comparison of light emission from *A. fumigatus* CBS144.89 (wild type; control), a reference reporter strain (Af C3) containing four copies of the nonoptimized luciferase reporter, and a new reporter strain (Af 2/7/1) that carries two copies of the codon-optimized luciferase gene. Wells of a white 96-well plate containing 200 μl potato dextrose broth (PDB) medium were inoculated in quadruplicate with 50,000 conidia of the respective strain and incubated for 13.5 h at 37°C. Luminescence was determined in a microplate reader after automatic injection of D-luciferin. The graph shows the relative light response units for a 0.5-s interval; data are means and standard deviations for four cultures. (B) Correlation of light emission and hyphal elongation. Bioluminescence was detected by using an IVIS 100 system, and hyphal elongation was determined microscopically using ImageJ software. Mean values and standard deviations for three independent cultures are shown.

notypic differences relative to the parental strain. Southern blot analysis revealed two copies of the luciferase gene construct that were stably integrated into the genome. When the luminescence of strain 2/7/1 was compared with that of the former reporter strain C3, luminescence was approximately 12 times more intense (Fig. 1A). In addition, taking into account that strain C3 contained four integrations of the luciferase gene construct, a significant increase in sensitivity was obtained by using the codon-optimized version of firefly luciferase.

Correlation of conidial germination with light emission of the reporter strain 2/7/1. To determine the kinetics of conidial germination and to correlate light emission of the reporter strain with the germination process, we cultured 5×10^5 conidia at 37°C in 24-well microplates containing 0.5 ml complete RPMI medium. From these cultures, microscopic pictures were recorded and analyzed by ImageJ software. Subsequently, luminescence was evaluated with an IVIS 100 system. The graph presented in Fig. 1B displays the increase of bioluminescence in correlation with hyphal elongation determined after 0, 5, 6, 8, 10, and 12 h of incubation.

Further incubation resulted in increased bioluminescence, but the correlation between light emission and hyphal elongation was difficult to assess (data not shown). This was due mainly to strong hyphal branching at 15 h rendering the evaluation of the total hyphal length difficult. Additionally, light scattering and quenching by overlaying hyphae could not be excluded in the bioluminescence reading. Thus, in subsequent *in vitro* antifungal drug assays with liquid cultures that used bioluminescence detection as a readout parameter, incubation times were mainly limited to the 10-h time point.

Comparison of antifungal susceptibilities of wild-type *A. fumigatus* and reporter strain 2/7/1 by standard techniques. To evaluate the drug susceptibility of the bioluminescent reporter strain 2/7/1 in comparison to its parental wild-type strain, two independent standard methods were used: MIC test strips and the microdilution method. Two methods were used because different *in vitro* susceptibility assays, such as the microdilution method, disc diffusion assays, and MIC test strips, sometimes show variances in MIC results (23–25). Drug susceptibility analyses with MIC test strips were performed for amphotericin B, voriconazole, posaconazole, anidulafungin, and caspofungin, whereas we limited analyses with the microdilution method to amphotericin B, voriconazole, and anidulafungin but additionally tested different combinations of these drugs. Due to possible microcolony formation on solid media with the use of MIC test strips (26), results were evaluated at 24 and 48 h, whereas results from microdilution were read after 48 h, as recommended in the EUCAST guidelines. Regardless of the test method, no significant differences in susceptibility were observed between the parental *A. fumigatus* wild-type strain CBS144.89 and the reporter strain 2/7/1 (Table 1). How-

TABLE 1 MIC determination by use of MIC test strips and the microdilution method

Strain	Time point (h)	Method	MIC (mg/liter)[a]				
			Amphotericin B	Voriconazole	Posaconazole	Anidulafungin	Caspofungin
Wild type	24	Test strip	0.125–0.19	0.064–0.094	0.047–0.064	0.004–0.006*	0.032*
	48	Test strip	1.5	0.094	0.094	0.006–0.008**	0.032–0.047**
2/7/1	24	Test strip	0.094–0.125	0.064–0.094	0.032–0.047	0.004–0.006*	0.032–0.047*
	48	Test strip	1.0–1.5	0.094	0.094	0.006–0.008**	0.047–0.064**
Wild type	48	Microdilution	1	0.25	ND	<0.032***	ND
2/7/1	48	Microdilution	1	0.25	ND	<0.032***	ND

[a] *, microcolonies were present in the inhibition zone; **, difficult to evaluate due to microcolonies; ***, data are MECs (at the lowest concentration tested, a hyperbranching phenotype of colonies was observed); ND, not determined.

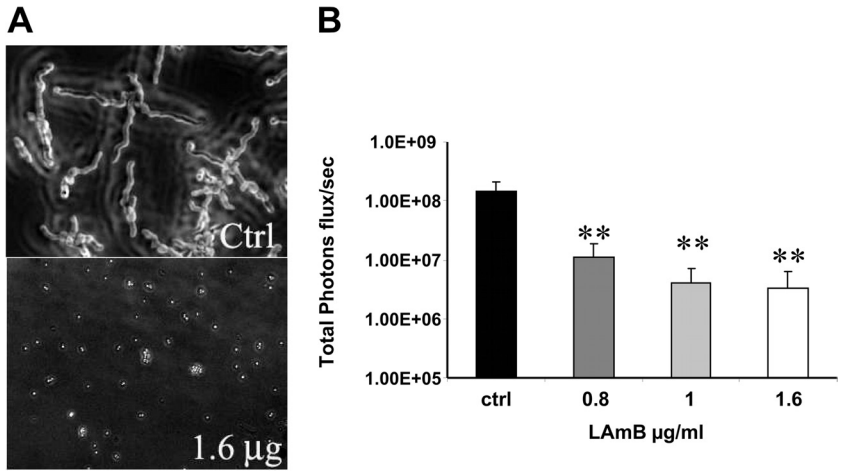

FIG 2 Effect of liposomal amphotericin B on growth of *A. fumigatus* in liquid cultures. (A) Conidia were cultured for 10 h at 37°C in the presence of increasing doses of liposomal amphotericin B (LAmB) ranging from 0.8 μg/ml to 1.6 μg/ml. The microscopic images show hyphal growth in the control culture, whereas LAmB at 1.6 μg/ml inhibited germination of conidia. (B) Conidia were cultured in triplicate ($n = 6$) to a final concentration of 5×10^5 conidia in 0.5 ml of complete RPMI medium and incubated for 10 h at 37°C. LAmB added at time zero significantly inhibited germination of conidia, and the luminescence decreased accordingly (**, $P < 0.05$).

ever, MIC values determined by the two independent methods were slightly different. Furthermore, while amphotericin B showed a low MIC value after 24 h (0.125 μg/ml) in the test strip analysis, the MIC increased by a factor of >10 within the next 24 h, due mainly to a fluffy nonsporulating mycelium that entered the previously formed inhibition zone, but the 48-h reading of MIC test strips was similar to the microdilution read at 48 h. In conclusion, regardless of the method used, all *in vitro* data indicated that the selected *A. fumigatus* reporter strain should be susceptible to all tested drugs under *in vivo* conditions.

Among drug combinations, synergistic effects were observed with the combination of amphotericin B and voriconazole. Although the drugs were added at sub-MIC levels that allowed normal mycelium formation in single use, stunted and highly branched colonies were observed with these combinations. This was especially true for amphotericin B at a fixed concentration of 0.25 mg/liter with voriconazole at concentrations down to 0.0625 mg/liter. However, no obvious effects of the combination of amphotericin B or voriconazole with anidulafungin were observed. These combinations revealed highly branched colonies that were similar in appearance to those with anidulafungin applied in single use.

Evaluation of drug susceptibility by microscopy and bioluminescence imaging. The analyses described above revealed that the bioluminescent reporter (i) showed similar drug susceptibility to that of the parental wild-type strain and (ii) showed a good correlation between bioluminescence and biomass formation in liquid cultures, at least when tested within the first 10 to 12 h after inoculation. To check whether bioluminescence determinations also allow correlation of the growth-inhibitory and toxic effects of antifungals with light emission, we performed susceptibility analyses in 24-well plates and evaluated growth microscopically, followed by quantification of bioluminescence intensity. For this purpose, different concentrations of liposomal amphotericin B, voriconazole, and anidulafungin were added at different time points and in different concentrations to conidia growing in complete RPMI medium.

(i) Liposomal amphotericin B. The inhibitory effect of liposomal amphotericin B was tested by culturing conidia for a total of 10 h in the presence of various amounts of the drug in the range of 0.8 μg/ml to 1.6 μg/ml. Microscopic evaluation showed that all concentrations strongly inhibited germination of conidia (Fig. 2A), and bioluminescence imaging (Fig. 2B) revealed that liposomal amphotericin B significantly ($P < 0.05$) reduced light emission at 0.8 μg/ml (92% inhibition), 1 μg/ml (97% inhibition), and 1.6 μg/ml (98% inhibition). These data are in good correlation with the results of the two standard susceptibility assays described above. However, since determinations of susceptibility by use of MIC test strips evaluated after 24 h indicated that even lower concentrations might be effective at early time points, we additionally tested lower concentrations (0.4, 0.2, and 0.02 μg/ml) of liposomal amphotericin B. In this case, a concentration of 0.2 μg/ml still resulted in 74% decreased bioluminescence, whereas no inhibition was observed with the lowest concentration (0.02 μg/ml) (data not shown).

In order to determine the drug efficacy in relation to the state of conidial germination, 0.8 μg of liposomal amphotericin B was added to germinating conidia at different time points. When liposomal amphotericin B was added at 0 h and maintained in the medium for 10 h, we observed 92% inhibition. When conidia were preincubated for either 5 or 4 h prior to liposomal amphotericin B addition and incubation was continued for a total of 10 h, bioluminescence determination revealed 88 or 92% inhibition, respectively. However, when conidia were pregerminated for 8 h prior to addition of amphotericin B and incubation was continued for another 2 h, no reduction in light emission in comparison to the control was observed. This indicates that efficient inhibition may occur only on either swollen or early-germinating conidia. Alternatively, the incubation time of 2 h in the presence of amphotericin B may have been too short to cause a significant inactivation of hyphae. Finally, to confirm a fungicidal activity of liposomal amphotericin B, conidia were incubated in the presence of the drug at 0.8 μg/ml for 10 h. Subsequently, cultures were washed and further incubated for 10 h at 37°C. Liposomal amphotericin B signif-

icantly inhibited germination of conidia, and determination of light emission revealed 99% inhibition in comparison to the control ($P < 0.05$). This experiment showed that liposomal amphotericin B was not only fungistatic but also fungicidal on *A. fumigatus* conidia.

(ii) Anidulafungin. Anidulafungin is a broad-spectrum echinocandin that inhibits fungal cell wall synthesis. MIC test strip analysis showed that low concentrations in the range of 4 to 8 ng/ml were effective. However, microcolonies formed on the plates and were also observed in the microdilution test, which is in agreement with a fungistatic rather than fungicidal effect of this drug (27).

To evaluate the correlation between light emission and growth in the presence of this drug, the same approach as that described for liposomal amphotericin B was followed. Compared to a control without drug, the addition of anidulafungin significantly inhibited the elongation of hyphae ($P < 0.05$) at 1 ng/ml (51% inhibition), 10 ng/ml (53% inhibition), and 100 ng/ml (55% inhibition), but evaluation of biomass formation by microscopic analysis was difficult due to hyperbranching of hyphal tips (not shown).

However, monitoring bioluminescence using the IVIS system showed that anidulafungin added at 0 h at concentrations of 1 and 10 ng/ml resulted in 25 and 26% inhibition of light emission, respectively. Similarly, addition of the drug at 100 ng/ml only slightly but significantly increased this inhibition, to 34% ($P < 0.05$). These data are in agreement with a high effectiveness of anidulafungin even at low concentrations but also show that germinated conidia are still alive due to the production of luciferase and ATP, which are both required for the light-emitting reaction during the oxidation of D-luciferin (13).

(iii) Voriconazole. Similar to liposomal amphotericin B, voriconazole targets the fungal cell membrane (28, 29) and is fungicidal against most *A. fumigatus* isolates (30). MIC testing by the two standard assays revealed effective concentrations in the range of 94 to 250 ng/ml at 48 h. Therefore, experiments with liquid cultures were performed at increasing doses of 1, 10, and 100 ng/ml, and incubation was performed for a total of 10 h.

Microscopic observations showed that no germination occurred in the presence of voriconazole at all three concentrations. However, the luminescence intensities indicate that not all conidia were killed during this treatment. Light emission was reduced by 85 to 86% for all three concentrations, which indicates that at least some active luciferase and ATP were still present. This is in agreement with results from microdilution, in which mycelial growth was observed at the 48-h time point for concentrations below 250 ng/ml.

***In vivo* drug efficacy in therapy of invasive aspergillosis.** Our *in vitro* studies confirmed the susceptibility of the bioluminescent *A. fumigatus* reporter strain against the important antifungals liposomal amphotericin B, voriconazole, and anidulafungin. However, the latter drug allowed initial germination of conidia that might hinder its use in monotherapy. In contrast, voriconazole and liposomal amphotericin B were highly efficient at preventing conidial germination and could be assumed to be highly effective under *in vivo* conditions. To address these questions and to visualize the power of bioluminescence imaging in reporting the efficacy of antifungals under *in vivo* conditions, therapy studies were performed on leukopenic mice. In the first approach, antifungal monotherapy was tested after pulmonary challenge of mice with different numbers of conidia, i.e., 5×10^5 and 2.5×10^5 conidia. Treatment was started at the time of infection and continued on a daily basis by intraperitoneal injection of the respective drug. Progression of infection or recovery was monitored by body weight determination and bioluminescence imaging.

Monotherapy with liposomal amphotericin B. Cyclophosphamide-treated mice were challenged with 5×10^5 or 2.5×10^5 conidia. The placebo groups received 5% glucose, and the treated group received liposomal amphotericin B (10 mg/kg/day). Treatment was given by intraperitoneal injection on a daily basis for 10 days, after which treatment was discontinued and mice were monitored for an additional 10 days to determine the level of fungal elimination. Following infection with the high infectious dose, the graphs presented in Fig. 3A illustrate (i) the correlation between the increase of bioluminescence signals and the weight loss during the first 6 days of infection in the placebo- and liposomal amphotericin B-treated groups of mice (data from a total of 15 animals for each group); and (ii) starting at day 4 postinfection, a significant difference between the treated and untreated groups for both bioluminescence signals ($P < 0.05$ at D4 and $P < 0.001$ at D6) and weight loss ($P < 0.05$ at D4 and $P < 0.01$ at D6). While body weight continued to decrease in the placebo group, the bioluminescence signal strongly increased. Furthermore, within this time frame, and regardless of the infectious dose, all placebo-treated animals succumbed to infection, with high luminescence signals. In contrast, in the treated group, only a transient increase in bioluminescence accompanied by a transient decrease in body weight was observed. Six days after infection, mice started to recover body weight and the bioluminescence decreased, reaching background levels of 1×10^5 total photons flux/s at day 20, when the experiment was terminated. Thus, treatment with liposomal amphotericin B had a beneficial effect on the outcome of infection at a high infectious dose.

A more detailed analysis of the development of bioluminescence signals is depicted in Fig. 3B. Regardless of treatment, weak and homogenous luminescence signals were detected from the sinus and lung regions of all mice early after infection, confirming successful infection. Furthermore, along with the expected bioluminescence signal increase from the lung region in placebo-treated animals, development of strong bioluminescence from the sinus region was common, especially at the infectious dose of 5×10^5 conidia. Interestingly, the sinus region also appeared as the major site of disease establishment in the liposomal amphotericin B-treated group, implying that liposomal amphotericin B has a higher therapeutic efficacy in the pulmonary region than in the sinus region. However, the majority of animals treated with liposomal amphotericin B showed only a transient increase of bioluminescence signals, and as stated above, the decrease in light emission was accompanied by a gain in weight. A similar pattern of luminescence decrease following infection was observed with the reduced dose of 2.5×10^5 conidia (data not shown).

In conclusion, liposomal amphotericin B had a strongly positive effect on life span and survival of treated mice and was effective at both infectious doses, with 80% of infected mice surviving the observation period (also see Fig. 4C).

Anidulafungin and voriconazole treatment at a high infectious dose. Similar to the liposomal amphotericin B treatment, in the first approach for anidulafungin and voriconazole, mice were challenged with 5×10^5 conidia and treated with either voriconazole or anidulafungin at a concentration of 10 mg/kg body weight

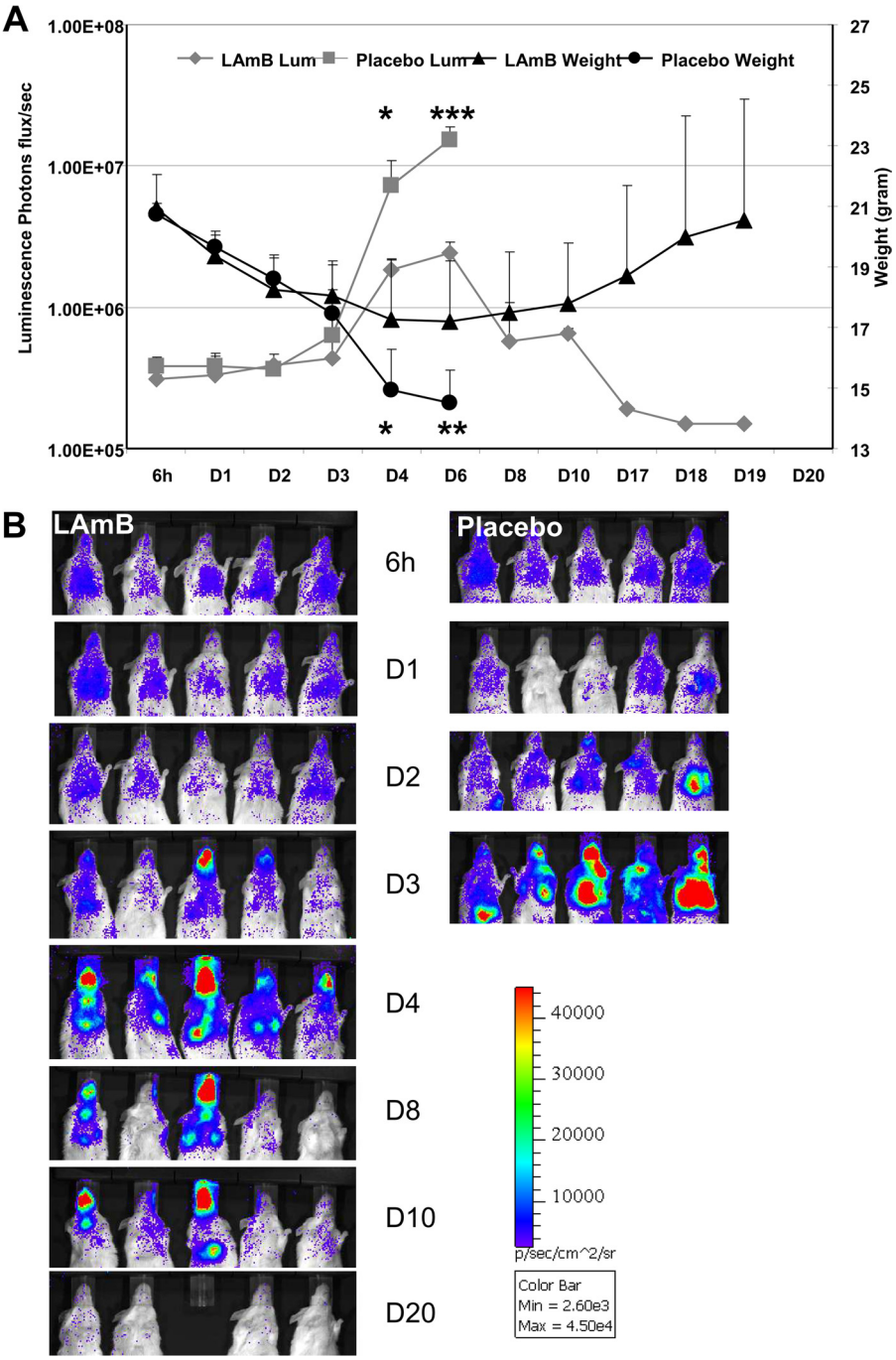

FIG 3 *In vivo* monitoring of liposomal amphotericin B efficacy in therapy of invasive pulmonary aspergillosis. (A) Immunosuppressed mice were infected with 5×10^5 conidia of *A. fumigatus* strain 2/7/1, and luminescence and body weight were monitored on a daily basis. The graphs for the LAmB-treated ($n = 15$) and placebo-treated ($n = 15$) groups show that increases in luminescence (gray) were concomitant with decreases in body weight (black). A significant difference concerning body weight and light emission ($P < 0.05$) between the treated and placebo groups was observed from D4 following infection. (B) Visualization of bioluminescence imaging exemplified for a representative group of LAmB- and placebo-treated mice. In survivors from the therapy group, luminescence decreased to background levels by 20 days postinfection. In contrast, luminescence strongly increased in the placebo group. Strong lung and sinus signals were predictive of the imminent death of mice.

for a total of 10 days. Control mice receiving the respective placebo treatment showed the development of luminescence signals and mortality described above. However, and unexpectedly, at this infectious dose, 90% of the treated animals developed severe signs of infection, loss of body weight, and increasing bioluminescence signals (Fig. 4A). Infected mice displayed signals from the lungs and also from the trachea, head, and sinus, indicating fungal invasion of these organs and suggesting a possible tracheitis, keratitis, and sinusitis. Infection at these sites was clearly visible even in the dorsal view for the treated and untreated groups (Fig. 4B).

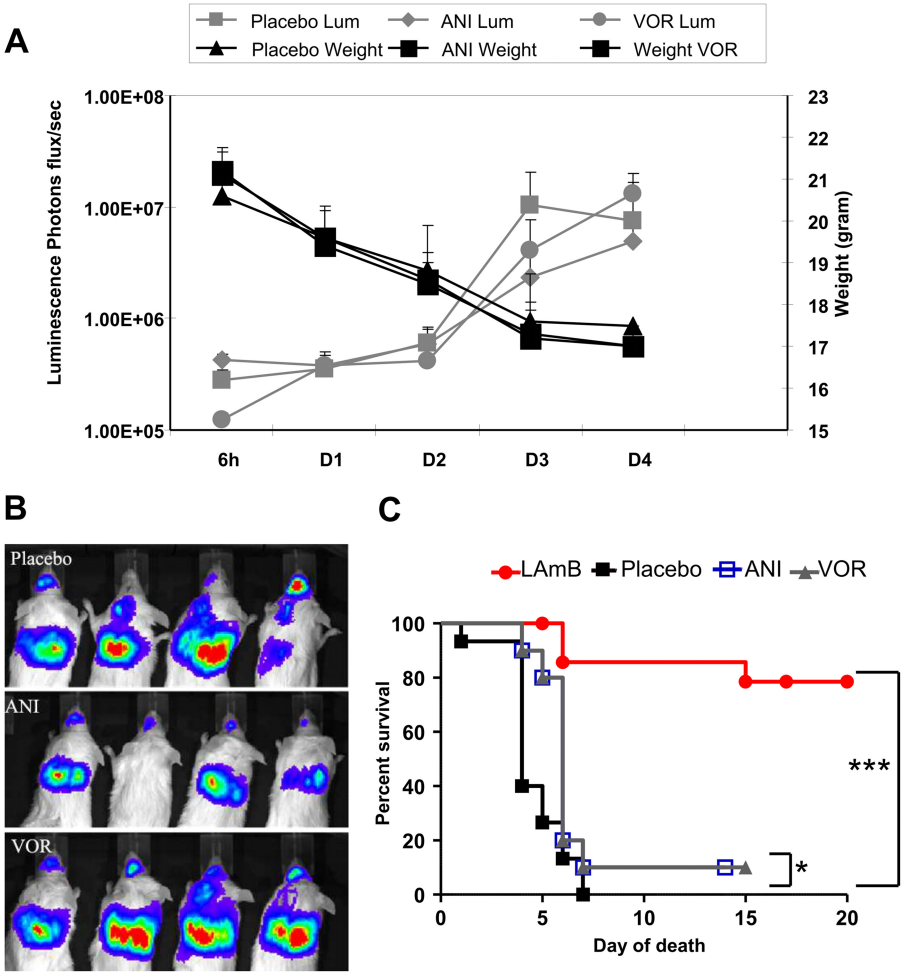

FIG 4 *In vivo* monitoring of anidulafungin and voriconazole efficacies in therapy of invasive pulmonary aspergillosis following infection with 5×10^5 conidia. (A) Immunosuppressed mice were infected with 5×10^5 conidia of *A. fumigatus* strain 2/7/1. Luminescence and weight were monitored daily for placebo ($n = 15$)-, anidulafungin (ANI; $n = 10$)-, and voriconazole (VOR; $n = 10$)-treated mice. Drugs (10 mg/kg/day) were administered daily. At this infectious dose, no difference was observed between the placebo-treated and therapy groups. The increase in luminescence was accompanied by a decrease in weight. (B) Luminescence images in dorsal view from a representative experiment with placebo-, ANI-, and VOR-treated mice 4 days after infection. Besides signals from the region of the lungs and trachea, luminescence from the head areas implies the development of severe sinusitis. (C) Analyses of survival rates of mice infected with 5×10^5 conidia following treatment with LAmB (also see Fig. 3), ANI, and VOR. Analyses were performed by Kaplan-Meier plots followed by the log rank (Mantel-Cox) test. *, $P < 0.05$; ***, $P < 0.001$.

Thus, among a total of 10 mice from each treated group at this high infectious dose, only 10% ($P < 0.05$) survived the infection (Fig. 4C). These results imply that either (i) bioavailability of voriconazole or anidulafungin after intraperitoneal injection was too low to efficiently inhibit fungal growth, (ii) both drugs were not effective in treatment of lung aspergillosis, or (iii) the fungal load was too high to allow for efficient therapy. To address these possibilities, a second therapy approach was performed, in which the infectious dose was lowered to 2.5×10^5 conidia per mouse.

Anidulafungin and voriconazole treatment at a reduced infectious dose. Despite the unsuccessful treatment of mice with anidulafungin or voriconazole at a high infectious dose, we repeated these treatment approaches but reduced the infectious dose to 2.5×10^5 conidia.

As observed in the above-described experiment with liposomal amphotericin B, the placebo-treated group rapidly succumbed to infection and displayed high luminescence signals (Fig. 5A). However, and in contrast to the case with the higher infectious dose, anidulafungin and voriconazole treatments significantly ($P < 0.0001$) reduced mortality rates (Fig. 5B). This result was particularly unexpected for anidulafungin, which allowed early germination of conidia under *in vitro* conditions. However, early germination was in agreement with a transient increase of luminescence until day 4 in all anidulafungin-treated animals (Fig. 5A). During the following days, 8 of 20 mice succumbed to infection, with high bioluminescence signals, as exemplified for mouse number 4 (M4) in Fig. 5A. A strong signal was also observed from a second mouse (M5), but this animal recovered from infection and showed no luminescence signal above background at day 17, when the experiment was terminated. Thus, the growth-inhibitory effect of anidulafungin on germinated conidia appears to be sufficient for therapy success at the reduced infectious dose.

Similarly, a significant improvement was also observed with voriconazole treatment. In the three mice shown as examples in

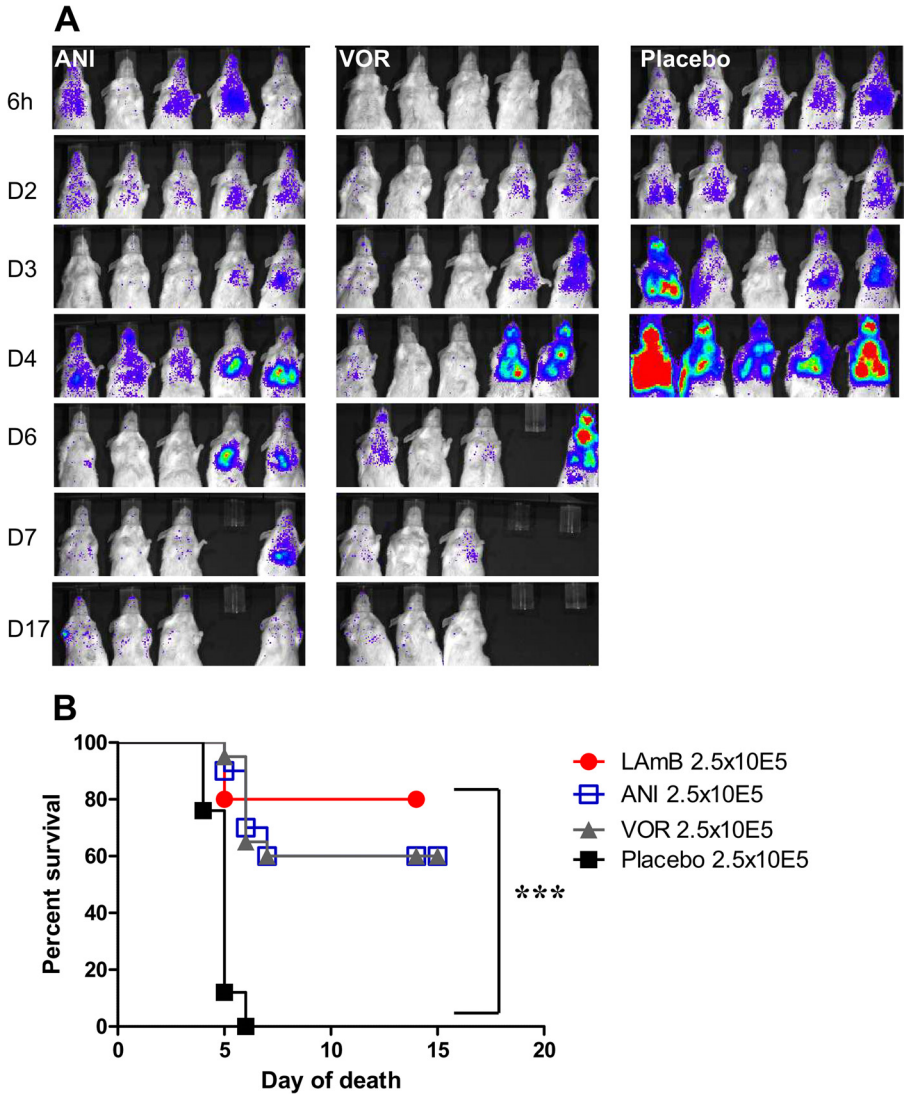

FIG 5 *In vivo* monitoring of anidulafungin and voriconazole efficacies in therapy of invasive pulmonary aspergillosis following infection with 2.5×10^5 conidia of strain 2/7/1. (A) Representative luminescence images of immunosuppressed mice infected with 2.5×10^5 conidia of *A. fumigatus* and treated with either anidulafungin (ANI), voriconazole (VOR), or a placebo. In comparison to the higher infectious dose (see Fig. 4), reduction of the infectious dose increased therapy efficacy, with partial to complete reduction of light emission from surviving animals. (B) Analyses of survival rates were performed by Kaplan-Meier plots followed by the log rank (Mantel-Cox) test for LAmB ($n = 10$), ANI ($n = 20$), and VOR ($n = 20$) treatments in comparison to the placebo group ($n = 25$) at the reduced infectious dose. For all drug treatments, a significant increase in survival (***, $P < 0.001$) was observed.

Fig. 5A, no strong increase in luminescence was observed for the duration of the treatment and the following observation period. This is in agreement with our *in vitro* results, which showed that voriconazole efficiently controlled conidial germination. However, as shown for the depicted group of mice, even at this reduced infectious dose, two mice (M4 and M5) revealed increasing bioluminescence signals and succumbed to infection on days 6 and 7, with signals from the lungs, trachea, and sinus (Fig. 5A). Thus, in total, 8 of 20 infected animals also succumbed to infection under this infection and treatment regimen.

In conclusion, in comparison to placebo-treated mice, which rapidly succumbed to infection even at the reduced infectious dose, treatment significantly improved survival for both drugs ($P < 0.0001$) (Fig. 5B). Treatment resulted in 60% survival following anidulafungin or voriconazole therapy, in contrast to 0% survival for the placebo group. However, to further improve therapy success, we investigated combination therapies in the reduced-dose infection model.

Combination treatments using the low-infectious-dose model of invasive pulmonary aspergillosis. To investigate the effect of combination therapy on treatment efficacy, we applied drugs in the following combinations: (i) 15 animals were treated with liposomal amphotericin B (10 mg/kg) in combination with anidulafungin (5 mg/kg), (ii) 10 animals were treated with liposomal amphotericin B (10 mg/kg) in combination with voriconazole (10 mg/kg), and (iii) 10 animals were treated with anidulafungin (5 mg/kg) in combination with voriconazole (10 mg/kg). Infection of cyclophosphamide-treated animals was performed with 2.5×10^5 conidia. The different drugs were given intraperitoneally and independently to mice.

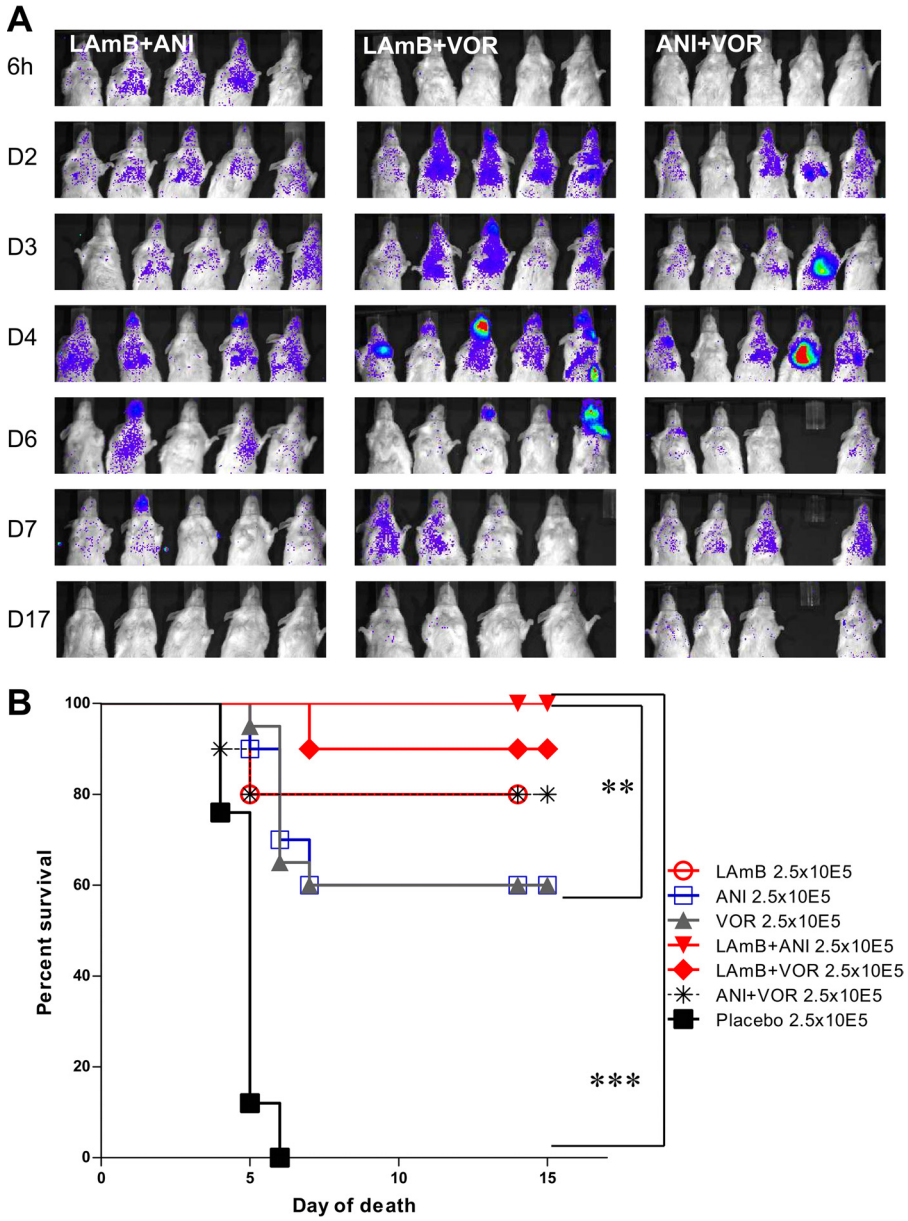

FIG 6 *In vivo* monitoring of the efficacy of drug combination treatments in therapy of invasive pulmonary aspergillosis following infection with 2.5×10^5 conidia of strain 2/7/1. (A) Representative luminescence images of immunosuppressed mice treated with combinations of liposomal amphotericin B (LAmB), anidulafungin (ANI), and voriconazole (VOR), as indicated. Mice surviving to day 6 showed full recovery, with light emission near background values. (B) Comparisons of all therapy approaches (single and combination treatments) at the reduced infectious dose. Analyses were performed by Kaplan-Meier plots followed by the log rank (Mantel-Cox) test. Monotherapy or combination therapy significantly improved the outcomes for the treatment group versus control group (***, $P < 0.0001$). Liposomal amphotericin B combined with anidulafungin significantly improved the outcome in comparison to that for mice treated only with anidulafungin (**, $P < 0.01$). Numbers of animals in groups were as follows: for LAmB + ANI, $n = 15$; for LAmB + VOR, $n = 10$; for VOR + ANI, $n = 10$; and for placebo, $n = 25$ (also see Fig. 5B).

Figure 6B presents Kaplan-Meier plots of cumulative mortality for the respective treatment groups in the combination study compared to monotherapy groups and untreated placebo controls. In comparison to placebo-treated mice ($P < 0.0001$) and monotherapy groups, the combination treatments significantly improved the outcome of infection. Although the concentration of anidulafungin in combination with liposomal amphotericin B was reduced to 5 mg/kg to avoid toxic side effects, this protocol significantly improved the survival, to 100% ($P < 0.01$) (Fig. 6B). Mice treated with this combination developed only mild signals from the sinus region and maintained near-background luminescence from the lung region (Fig. 6A). This implies that this combination reduced fungal growth not only at pulmonary regions but also at extrapulmonary sites, without obvious major adverse side effects.

When liposomal amphotericin B was combined with voriconazole, survival increased from 60% for voriconazole monotherapy to 90%, but this combination appeared to be not signifi-

cantly superior to liposomal amphotericin B monotherapy, which showed 80% survival. As shown in Fig. 6A, a transient increase in bioluminescence was observed, especially at extrapulmonary sites such as the trachea and sinuses (depicted in M1, M3, and M5). However, in M1 and M3, these signals decreased with ongoing therapy, indicating the efficacy of this combination.

Finally, when anidulafungin at 5 mg/kg was combined with voriconazole at 10 mg/kg, survival of mice also increased to 80%, in comparison to 60% for monotherapy for both drugs. Although signals from the sinus generally remained very low, individual mice (exemplified for M4 in Fig. 6A) developed strong lung signals and succumbed to infection.

From these experiments, we concluded that following infection with the reduced dose of conidia and in comparison to placebo-treated mice, which all succumbed to infection, (i) no antagonism was observed following the combinations; (ii) all combination treatments improved survival; and (iii) in this murine model, the best results were obtained following the combination of liposomal amphotericin B with anidulafungin ($P < 0.01$ compared to liposomal amphotericin B monotherapy).

Histopathology. For histopathological analysis, we considered the control (placebo) group and six treatment conditions: anidulafungin, liposomal amphotericin B, and voriconazole as monotherapies as well as liposomal amphotericin B plus anidulafungin, anidulafungin plus voriconazole, and liposomal amphotericin B plus voriconazole as combination therapies. Control mice that did not receive any treatment died within 6 days after inoculation (inoculation dose, 2.5×10^5 conidia). These mice displayed marked to severe pulmonary lesions characterized by multifocal to coalescent infiltrations of neutrophils and macrophages associated with bronchiolar and alveolar epithelial cell necrosis and vascular phenomena (necrosis, thrombi, and hemorrhages). Within these lesions, we identified a high density of hyphae (Fig. 7). In contrast, mice under therapy that survived the observation period were euthanized between days 17 and 20. Pulmonary lesions were heterogenous in the different treated groups, varying from no visible lesions to infiltrates of mononucleated cells or abscesses and granulomas. However, the overall density of intralesional hyphae was markedly decreased. Among the different conditions, two treatments, i.e., liposomal amphotericin B in combination with either voriconazole or anidulafungin, appeared superior to the other treatment regimens. These treatments resulted in an absence of significant histological lesions and fungal elements in the observed tissue sections (Fig. 7).

DISCUSSION

In this study, we generated a bioluminescent *A. fumigatus* strain expressing a codon-optimized version of firefly luciferase. As previously described for the use of a codon-adapted synthetic version of firefly luciferase in research on *Neurospora crassa* (31), codon adaptation significantly increased light emission in *A. fumigatus* as well. This optimization resulted in increased sensitivity of the reporter system in both *in vitro* and *in vivo* experiments compared to that of a strain carrying a luciferase gene codon adapted for expression in mammalian cells (17, 18). Since the selected reporter strain, strain 2/7/1, revealed no phenotypic growth defects, it appeared to be suitable to investigate the effectiveness of antifungals under *in vivo* conditions. Indeed, the bioluminescent reporter strain enabled real-time monitoring of infection after intranasal inhalation of conidia. Bioluminescence detection visualized not

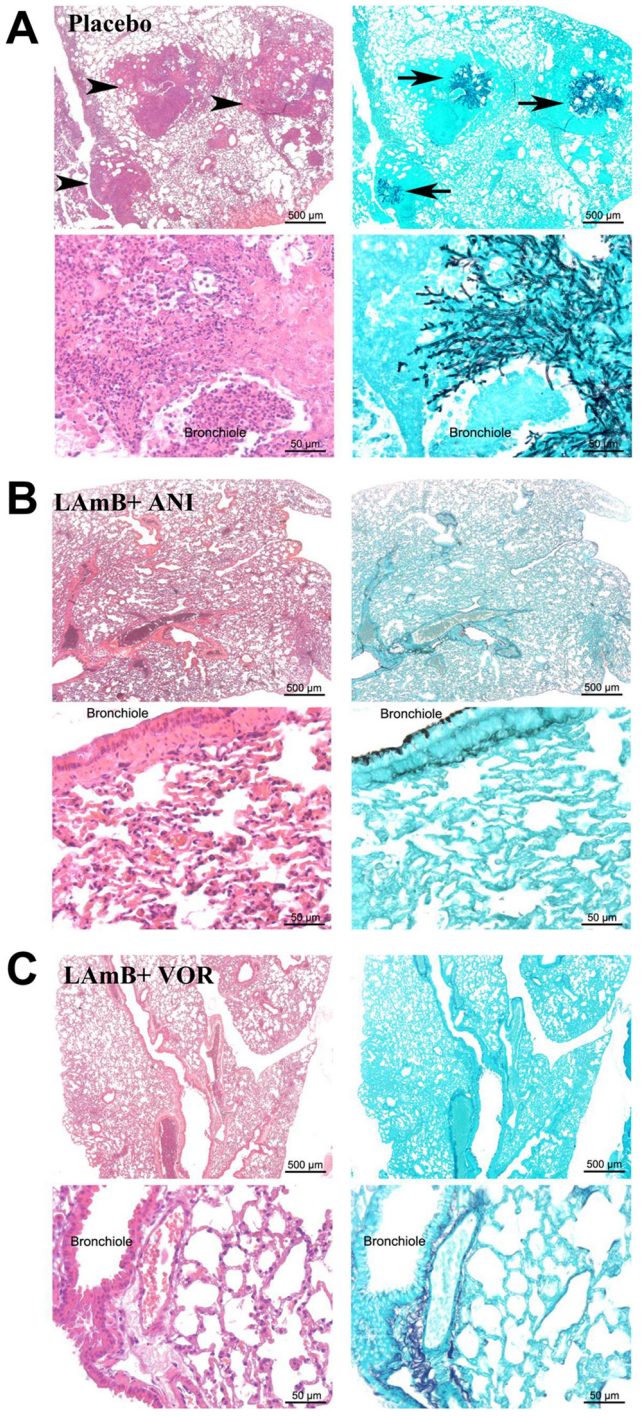

FIG 7 Lung histology of mice infected with 2.5×10^5 conidia of strain 2/7/1. Representative images of the placebo group 6 days after infection (A) and of the groups receiving combination treatment with liposomal amphotericin B (LAmB) and anidulafungin (ANI) (B) or LAmB and voriconazole (VOR) (C) are shown. Surviving animals from the combination treatment groups were euthanized at day 17 postinfection. (Left) Hematoxylin-eosin (HE) staining. (Right) Grocott's methenamine silver staining. Placebo-treated mice displayed multifocal pulmonary inflammatory lesions (arrowheads) containing a high density of fungi (arrows) and were characterized by multifocal infiltrates of macrophages and neutrophils filling bronchiolar spaces and extending to alveoli, associated with necrosis of epithelial cells and hemorrhages (magnification of HE staining). LAmB-ANI- and LAmB-VOR-treated mice did not display significant histological lesions or fungal elements at D17 postinfection.

only lung infections but also infections at extrapulmonary sites, such as the sinus or the trachea, and also visualized the kinetics of disease progression in individual animals. For placebo-treated mice challenged with either a high or reduced dose of conidia, mice succumbed to infection within 4 to 6 days, accompanied by increasing bioluminescence signals from the sinus region, trachea, and lungs. Therefore, this system appeared to be well suited for studying antifungal therapy approaches.

Liposomal amphotericin B (32, 33) and voriconazole (34–36) are common drugs in prophylactic use to prevent fungal infections in high-risk patients, although treatment failure and breakthrough of invasive fungal infections have been observed (2, 37, 38). Furthermore, echinocandins generally show good *in vitro* effectiveness against *Candida* and *Aspergillus* species, and several retrospective studies on the efficacies of micafungin and caspofungin in prophylactic and therapeutic approaches showed similar efficacies to those observed for various azoles and amphotericin B (39). However, due to the lack of large randomized trial studies, the use of these antifungals in primary prophylaxis has not yet been recommended. This is especially true for anidulafungin, which was approved only recently: in 2006 in the United States and in 2007 in Europe (39). Thus, reports on the efficacy of this drug are rather limited.

Although our analyses revealed that liposomal amphotericin B, anidulafungin, and voriconazole had good *in vitro* activities against *A. fumigatus*, only liposomal amphotericin B was highly effective in monotherapy, regardless of the infectious dose administered. However, breakthrough of infection was observed in some cases, especially following infection with the high dose of conidia. In this situation, disease manifestation was limited mostly to the trachea and sinuses, whereas lung signals remained generally low in all animals. This implies that amphotericin B might display a reduced bioavailability within the sinus region. This is in agreement with an investigation in which the efficacies of liposomal and conventional amphotericin B were compared in therapy of sinus infections. Although liposomal formulations appeared superior to conventional amphotericin B, treatment success remained low, at 50%, compared to 18.8% with the conventional formulation (37). However, it needs to be mentioned that the patient populations studied were significantly different, which might have caused the better outcome with the liposomal formulation. Nevertheless, in our analyses, the bioluminescence signals from the sinus region for liposomal amphotericin B treatment support the idea that extrapulmonary bioavailability, even that of lipid formulations, might be low. However, 80% of mice survived infection with liposomal amphotericin B treatment, with a complete clearance of the luminescence signal between days 17 and 20, which supports the suitability of this drug for primary therapy of pulmonary aspergillosis.

In contrast to the case for liposomal amphotericin B, treatment success with voriconazole and anidulafungin was highly dependent on the infectious dose. While both drugs nearly completely failed when the higher infectious dose was used, the success rate increased significantly with the reduced dose. The treatment failure with anidulafungin at the high infectious dose is consistent with the results obtained for a model of experimental pulmonary aspergillosis in neutropenic rabbits that were challenged with 4 times the amount of inoculum given in this study. Under therapy with anidulafungin at 10 mg/kg/day, only 18% of animals survived (40). A recent analysis of the pharmacokinetics of anidulafungin in mice revealed a good correlation of serum level with the applied dose, which indicates that an effective concentration in serum can be achieved (41). However, the same study showed that although therapy success increased with increasing dosages of the drug, the maximum response was not obtained, even at 20 mg/kg. Furthermore, increasing the dose to 40 mg/kg caused toxic side effects (41). In our study, we did not increase the anidulafungin concentration but slightly reduced the fungal load by maintaining 100% mortality in the control group. This reduction caused significantly less invasive growth in a majority of mice and allowed the recurring immune system to clear the infection in 60% of infected animals.

Concerning voriconazole, the situation appears different, although the treatment success was comparable to that with anidulafungin. Although some studies reported a response rate of only 50% for voriconazole for therapy of pulmonary disease (40), the good *in vitro* effectiveness against the tested *A. fumigatus* strain should have resulted in a higher *in vivo* efficacy. The main problem in the use of voriconazole in the murine system seems to derive from rapid inactivation by cytochrome P450, which is autoinduced by voriconazole in mice (42). Therefore, specific feeding conditions, such as the addition of grapefruit juice to the drinking water (43), seem to be required to study the effectiveness of this drug in the murine system. Therefore, care has to be taken in the interpretation of therapy efficacy in our models. However, in agreement with the assumption of low bioavailability, voriconazole was effective at the lower infectious dose, as some animals survived, without development of high bioluminescence signals.

Another aim of our study was to investigate the success of combination therapy. Combination therapy with echinocandins and triazoles or polyenes and echinocandins has been assumed to be more active for therapy of invasive aspergillosis than therapy with a single agent (44, 45). However, although not followed in our study, it seems important to monitor blood markers for hepato- and nephrotoxicity. When we tried to increase the anidulafungin concentration in combination with liposomal amphotericin B to 20 mg/kg/day, rapid death of mice occurred, indicating the occurrence of severe complications from either drug (data not shown).

However, when we reduced the anidulafungin concentration to 5 mg/kg/day, synergistic interactions between anidulafungin and voriconazole and between anidulafungin and liposomal amphotericin B were observed. The latter combination led to 100% survival, with only low transient increases of bioluminescence from the lungs and sinuses. With respect to our *in vitro* data, we assume that a potentially broadened bioavailability of drugs at all body sites might have caused this synergism, rather than a direct synergistic effect of both drugs on individual fungal cells. Mice treated with liposomal amphotericin B monotherapy suffered mainly from histologically confirmed sinus infections (data not shown), whereas anidulafungin monotherapy frequently resulted in high signals from the pulmonary tract. The combination of both drugs controlled infection at both sites, resulting in 100% survival. Thus, combination therapy might indeed help to combat life-threatening infections if the side effects are tolerated by patients.

Interestingly, despite the presumably low bioavailability of voriconazole due to its rapid inactivation in the murine system, we also observed efficacy of liposomal amphotericin B combined

with voriconazole in the setting of invasive pulmonary aspergillosis in the murine model. This is in contrast to a potential antagonism that was observed for the combination of ravuconazole with liposomal amphotericin B in a rabbit model of invasive pulmonary aspergillosis (46). Antagonistic effects were also observed with combination therapy of *C. albicans* sepsis with amphotericin B and itraconazole, since the combination was strongly inferior to amphotericin B monotherapy (47). Thus, it remains unclear whether our improvement derived from the use of a different azole or was observed only because of the low bioavailability of voriconazole in our model, reducing toxic and antagonistic effects. However, our *in vitro* combination experiment at least showed that amphotericin B in combination with voriconazole, both given at sub-MIC levels, displayed a synergistic effect. Furthermore, examples of successful combination therapy with voriconazole and lipid formulations of amphotericin B were also given for experimental murine central nervous system (CNS) aspergillosis (44, 48). Additionally, recent data published on the exposure of patients to voriconazole and liposomal amphotericin B showed no antagonism of these drugs, at least when given sequentially (49).

In summary, bioluminescence imaging strongly refines animal models by providing detailed spatial and temporal information on disease progression from diverse body sites. Due to the repeated imaging of individual animals, the total number of animals required to draw conclusions can be reduced significantly. In all our studies, a strong increase in the bioluminescence signal correlated with breakthrough infections and eventual death of animals. Therefore, bioluminescence imaging in addition to body weight determination can be used as a suitable marker for predicting treatment efficacy in future experiments. Just recently, bioluminescent reporter strains were also generated for *Aspergillus terreus* and revealed insights on disease establishment of invasive pulmonary aspergillosis dependent on the immunosuppressive regimen (50). Furthermore, bioluminescent *Fusarium* strains and improved bioluminescent *C. albicans* strains have been generated that are under investigation for their suitability for monitoring invasive fungal infections (unpublished data). This set of fungal species will allow us to test new therapy approaches on a broad range of important fungal pathogens.

The current study on *A. fumigatus* in the setting of invasive aspergillosis shows that (i) even if drugs are given intraperitoneally, the distribution of drugs to different sites of infection is possible; (ii) depending on their bioavailability, some drugs seem able to control only moderate fungal burdens under *in vivo* conditions; and (iii) the infectious dose used in model systems can strongly influence the results. Our data also imply that the efficacy of treatment relies on the experimental model system applied. Different organs are targeted depending on the route of infection, e.g., systemic infection, intracerebral injection, or intranasal infection. Bioluminescence imaging may provide a more detailed analysis of drug efficacy in different target organs and should therefore be considered in future antifungal testing.

ACKNOWLEDGMENTS

This work was supported by Contrats de Recherche grants from Gilead and Pfizer.

We thank Marie-Anne Nicola from Imagopole and T. Angélique from the animal facilities for their assistance.

REFERENCES

1. **Patterson TF, Kirkpatrick WR, White M, Hiemenz JW, Wingard JR, Dupont B, Rinaldi MG, Stevens DA, Graybill JR.** 2000. Invasive aspergillosis. Disease spectrum, treatment practices, and outcomes. Medicine (Baltimore, MD) **79**:250–260.
2. **Paterson PJ, Seaton S, Prentice HG, Kibbler CC.** 2003. Treatment failure in invasive aspergillosis: susceptibility of deep tissue isolates following treatment with amphotericin B. J. Antimicrob. Chemother. **52**:873–876.
3. **Stevens DA, Schwartz HJ, Lee JY, Moskovitz BL, Jerome DC, Catanzaro A, Bamberger DM, Weinmann AJ, Tuazon CU, Judson MA, Platts-Mills TA, DeGraff AC, Jr.** 2000. A randomized trial of itraconazole in allergic bronchopulmonary aspergillosis. N. Engl. J. Med. **342**:756–762.
4. **Metcalf SC, Dockrell DH.** 2007. Improved outcomes associated with advances in therapy for invasive fungal infections in immunocompromised hosts. J. Infect. **55**:287–299.
5. **Goto N, Hara T, Tsurumi H, Ogawa K, Kitagawa J, Kanemura N, Kasahara S, Yamada T, Shimizu M, Nakamura M, Matsuura K, Moriwaki H.** 2010. Efficacy and safety of micafungin for treating febrile neutropenia in hematological malignancies. Am. J. Hematol. **85**:872–876.
6. **Herbrecht R, Maertens J, Baila L, Aoun M, Heinz W, Martino R, Schwartz S, Ullmann AJ, Meert L, Paesmans M, Marchetti O, Akan H, Ameye L, Shivaprakash M, Viscoli C.** 2010. Caspofungin first-line therapy for invasive aspergillosis in allogeneic hematopoietic stem cell transplant patients: an European Organisation for Research and Treatment of Cancer study. Bone Marrow Transplant. **45**:1227–1233.
7. **Sarfati J, Diaquin M, Debeaupuis JP, Schmidt A, Lecaque D, Beauvais A, Latge JP.** 2002. A new experimental murine aspergillosis model to identify strains of *Aspergillus fumigatus* with reduced virulence. Nihon Ishinkin Gakkai Zasshi **43**:203–213.
8. **Kousha M, Tadi R, Soubani AO.** 2011. Pulmonary aspergillosis: a clinical review. Eur. Respir. Rev. **20**:156–174.
9. **Balloy V, Huerre M, Latge JP, Chignard M.** 2005. Differences in patterns of infection and inflammation for corticosteroid treatment and chemotherapy in experimental invasive pulmonary aspergillosis. Infect. Immun. **73**:494–503.
10. **Montagnoli C, Bozza S, Gaziano R, Zelante T, Bonifazi P, Moretti S, Bellocchio S, Pitzurra L, Romani L.** 2006. Immunity and tolerance to *Aspergillus fumigatus*. Novartis Found. Symp. **279**:66–77.
11. **Sheppard DC, Graybill JR, Najvar LK, Chiang LY, Doedt T, Kirkpatrick WR, Bocanegra R, Vallor AC, Patterson TF, Filler SG.** 2006. Standardization of an experimental murine model of invasive pulmonary aspergillosis. Antimicrob. Agents Chemother. **50**:3501–3503.
12. **Andreu N, Zelmer A, Wiles S.** 2011. Noninvasive biophotonic imaging for studies of infectious disease. FEMS Microbiol. Rev. **35**:360–394.
13. **Brock M.** 2012. Application of bioluminescence imaging for in vivo monitoring of fungal infections. Int. J. Microbiol. **2012**:956794. doi:10.1155/2012/956794.
14. **Hutchens M, Luker GD.** 2007. Applications of bioluminescence imaging to the study of infectious diseases. Cell. Microbiol. **9**:2315–2322.
15. **Doyle TC, Nawotka KA, Purchio AF, Akin AR, Francis KP, Contag PR.** 2006. Expression of firefly luciferase in *Candida albicans* and its use in the selection of stable transformants. Microb. Pathog. **40**:69–81.
16. **Doyle TC, Nawotka KA, Kawahara CB, Francis KP, Contag PR.** 2006. Visualizing fungal infections in living mice using bioluminescent pathogenic *Candida albicans* strains transformed with the firefly luciferase gene. Microb. Pathog. **40**:82–90.
17. **Brock M, Jouvion G, Droin-Bergere S, Dussurget O, Nicola MA, Ibrahim-Granet O.** 2008. Bioluminescent *Aspergillus fumigatus*, a new tool for drug efficiency testing and in vivo monitoring of invasive aspergillosis. Appl. Environ. Microbiol. **74**:7023–7035.
18. **Ibrahim-Granet O, Jouvion G, Hohl TM, Droin-Bergere S, Philippart F, Kim OY, Adib-Conquy M, Schwendener R, Cavaillon JM, Brock M.** 2010. In vivo bioluminescence imaging and histopathopathologic analysis reveal distinct roles for resident and recruited immune effector cells in defense against invasive aspergillosis. BMC Microbiol. **10**:105. doi:10.1186/1471-2180-10-105.
19. **Jouvion G, Brock M, Droin-Bergere S, Ibrahim-Granet O.** 2012. Duality of liver and kidney lesions after systemic infection of immunosuppressed and immunocompetent mice with *Aspergillus fumigatus*. Virulence **3**:43–50.
20. **Szekely A, Johnson EM, Warnock DW.** 1999. Comparison of E-test and

broth microdilution methods for antifungal drug susceptibility testing of molds. J. Clin. Microbiol. **37**:1480–1483.
21. **Cuenca-Estrella M, Arendrup MC, Chryssanthou E, Dannaoui E, Lass-Florl C, Sandven P, Velegraki A, Rodriguez-Tudela JL.** 2007. Multicentre determination of quality control strains and quality control ranges for antifungal susceptibility testing of yeasts and filamentous fungi using the methods of the Antifungal Susceptibility Testing Subcommittee of the European Committee on Antimicrobial Susceptibility Testing (AFST-EUCAST). Clin. Microbiol. Infect. **13**:1018–1022.
22. **Sinha BK, Monga DP, Prasad S.** 1988. A combination of Gomori-Grocott methenamine silver nitrate and hematoxylene and eosin staining technique for the demonstration of *Candida albicans* in tissue. Quad. Sclavo Diagn. **24**:129–132.
23. **Johnson EM.** 2008. Issues in antifungal susceptibility testing. J. Antimicrob. Chemother. **61**(Suppl 1):i13–i18.
24. **Pfaller MA, Messer SA, Mills K, Bolmstrom A.** 2000. In vitro susceptibility testing of filamentous fungi: comparison of Etest and reference microdilution methods for determining itraconazole MICs. J. Clin. Microbiol. **38**:3359–3361.
25. **Pfaller MA, Messer SA, Boyken L, Hollis RJ, Diekema DJ.** 2003. In vitro susceptibility testing of filamentous fungi: comparison of Etest and reference M38-A microdilution methods for determining posaconazole MICs. Diagn. Microbiol. Infect. Dis. **45**:241–244.
26. **Martos AI, Romero A, Gonzalez MT, Gonzalez A, Serrano C, Castro C, Peman J, Canton E, Martin-Mazuelos E.** 2010. Evaluation of the Etest method for susceptibility testing of *Aspergillus* spp. and *Fusarium* spp. to three echinocandins. Med. Mycol. **48**:858–861.
27. **Odds FC, Brown AJ, Gow NA.** 2003. Antifungal agents: mechanisms of action. Trends Microbiol. **11**:272–279.
28. **Martinez LR, Ntiamoah P, Gacser A, Casadevall A, Nosanchuk JD.** 2007. Voriconazole inhibits melanization in *Cryptococcus neoformans*. Antimicrob. Agents Chemother. **51**:4396–4400.
29. **Van Epps HL, Feldmesser M, Pamer EG.** 2003. Voriconazole inhibits fungal growth without impairing antigen presentation or T-cell activation. Antimicrob. Agents Chemother. **47**:1818–1823.
30. **Martin MV, Yates J, Hitchcock CA.** 1997. Comparison of voriconazole (UK-109,496) and itraconazole in prevention and treatment of *Aspergillus fumigatus* endocarditis in guinea pigs. Antimicrob. Agents Chemother. **41**:13–16.
31. **Gooch VD, Mehra A, Larrondo LF, Fox J, Touroutoutoudis M, Loros JJ, Dunlap JC.** 2008. Fully codon-optimized luciferase uncovers novel temperature characteristics of the *Neurospora* clock. Eukaryot. Cell **7**:28–37.
32. **Adler-Moore J, Proffitt RT.** 2002. AmBisome: liposomal formulation, structure, mechanism of action and pre-clinical experience. J. Antimicrob. Chemother. **49**(Suppl 1):21–30.
33. **Olson JA, George A, Constable D, Smith P, Proffitt RT, Adler-Moore JP.** 2010. Liposomal amphotericin B and echinocandins as monotherapy or sequential or concomitant therapy in murine disseminated and pulmonary *Aspergillus fumigatus* infections. Antimicrob. Agents Chemother. **54**: 3884–3894.
34. **Gergis U, Markey K, Greene J, Kharfan-Dabaja M, Field T, Wetzstein G, Schell MJ, Huang Y, Anasetti C, Perkins J.** 2010. Voriconazole provides effective prophylaxis for invasive fungal infection in patients receiving glucocorticoid therapy for GVHD. Bone Marrow Transplant. **45**: 662–667.
35. **Cordonnier C, Rovira M, Maertens J, Olavarria E, Faucher C, Bilger K, Pigneux A, Cornely OA, Ullmann AJ, Bofarull RM, de la Camara R, Weisser M, Liakopoulou E, Abecasis M, Heussel CP, Pineau M, Ljungman P, Einsele H.** 2010. Voriconazole for secondary prophylaxis of invasive fungal infections in allogeneic stem cell transplant recipients: results of the VOSIFI study. Haematologicaae **95**:1762–1768.
36. **Cadena J, Levine DJ, Angel LF, Maxwell PR, Brady R, Sanchez JF, Michalek JE, Levine SM, Restrepo MI.** 2009. Antifungal prophylaxis with voriconazole or itraconazole in lung transplant recipients: hepatotoxicity and effectiveness. Am. J. Transplant. **9**:2085–2091.
37. **White MH, Anaissie EJ, Kusne S, Wingard JR, Hiemenz JW, Cantor A, Gurwith M, Du Mond C, Mamelok RD, Bowden RA.** 1997. Amphotericin B colloidal dispersion vs. amphotericin B as therapy for invasive aspergillosis. Clin. Infect. Dis. **24**:635–642.
38. **Denning DW, Ribaud P, Milpied N, Caillot D, Herbrecht R, Thiel E, Haas A, Ruhnke M, Lode H.** 2002. Efficacy and safety of voriconazole in the treatment of acute invasive aspergillosis. Clin. Infect. Dis. **34**:563–571.
39. **Mikulska M, Viscoli C.** 2011. Current role of echinocandins in the management of invasive aspergillosis. Curr. Infect. Dis. Rep. **13**:517–527.
40. **Petraitis V, Petraitiene R, Hope WW, Meletiadis J, Mickiene D, Hughes JE, Cotton MP, Stergiopoulou T, Kasai M, Francesconi A, Schaufele RL, Sein T, Avila NA, Bacher J, Walsh TJ.** 2009. Combination therapy in treatment of experimental pulmonary aspergillosis: in vitro and in vivo correlations of the concentration- and dose-dependent interactions between anidulafungin and voriconazole by Bliss independence drug interaction analysis. Antimicrob. Agents Chemother. **53**:2382–2391.
41. **Seyedmousavi S, Bruggemann RJ, Melchers WJ, Verweij PE, Mouton JW.** 2013. Pharmacodynamics of anidulafungin against clinical *Aspergillus fumigatus* isolates in a nonneutropenic murine model of disseminated aspergillosis. Antimicrob. Agents Chemother. **57**:303–308.
42. **Roffey SJ, Cole S, Comby P, Gibson D, Jezequel SG, Nedderman AN, Smith DA, Walker DK, Wood N.** 2003. The disposition of voriconazole in mouse, rat, rabbit, guinea pig, dog, and human. Drug Metab. Dispos. **31**:731–741.
43. **Sugar AM, Liu XP.** 2000. Effect of grapefruit juice on serum voriconazole concentrations in the mouse. Med. Mycol. **38**:209–212.
44. **Clemons KV, Espiritu M, Parmar R, Stevens DA.** 2005. Comparative efficacies of conventional amphotericin B, liposomal amphotericin B (AmBisome), caspofungin, micafungin, and voriconazole alone and in combination against experimental murine central nervous system aspergillosis. Antimicrob. Agents Chemother. **49**:4867–4875.
45. **Johnson MD, MacDougall C, Ostrosky-Zeichner L, Perfect JR, Rex JH.** 2004. Combination antifungal therapy. Antimicrob. Agents Chemother. **48**:693–715.
46. **Meletiadis J, Petraitis V, Petraitiene R, Lin P, Stergiopoulou T, Kelaher AM, Sein T, Schaufele RL, Bacher J, Walsh TJ.** 2006. Triazole-polyene antagonism in experimental invasive pulmonary aspergillosis: in vitro and in vivo correlation. J. Infect. Dis. **194**:1008–1018.
47. **Sugar AM, Liu XP.** 1998. Interactions of itraconazole with amphotericin B in the treatment of murine invasive candidiasis. J. Infect. Dis. **177**:1660–1663.
48. **Clemons KV, Parmar R, Martinez M, Stevens DA.** 2006. Efficacy of Abelcet alone, or in combination therapy, against experimental central nervous system aspergillosis. J. Antimicrob. Chemother. **58**:466–469.
49. **Cornely OA, Maertens J, Bresnik M, Ullmann AJ, Ebrahimi R, Herbrecht R.** 2010. Treatment outcome of invasive mould disease after sequential exposure to azoles and liposomal amphotericin B. J. Antimicrob. Chemother. **65**:114–117.
50. **Slesiona S, Ibrahim-Granet O, Olias P, Brock M, Jacobsen ID.** 2012. Murine infection models for *Aspergillus terreus* pulmonary aspergillosis reveal long-term persistence of conidia and liver degeneration. J. Infect. Dis. **205**:1268–1277.